The CMB power spectrum at $\ell = 30 - 200$ from QMASK

Yongzhong Xu, Max Tegmark, Angelica de Oliveira-Costa
Dept. of Physics, Univ. of Pennsylvania, Philadelphia, PA 19104; xuyz@physics.upenn.edu
(Submitted to Phys. Rev. D May 1 2001, accepted Jan 15 2002)

We measure the cosmic microwave background (CMB) power spectrum on angular scales $\ell \sim 30 - 200$ ($1^\circ - 6^\circ$) from the QMASK map, which combines the data from the QMAP and Saskatoon experiments. Since the accuracy of recent measurements leftward of the first acoustic peak is limited by sample-variance, the large area of the QMASK map (648 square degrees) allows us to place among the sharpest constraints to date in this range, in good agreement with BOOMERanG and (on the largest scales) COBE/DMR. By band-pass-filtering the QMAP and Saskatoon maps, we are able to spatially compare them scale-by-scale to check for beam- and pointing-related systematic errors.

I. INTRODUCTION

After the discovery of large-scale Cosmic Microwave Background (CMB) fluctuations by the COBE satellite [1], experimental groups have forged ahead to probe ever smaller scales. Now that TOCO [2,3], BOOMERanG [4] and Maxima [5] have convincingly measured the location and height of the first acoustic peak, attention is shifting to still smaller scales to resolve outstanding theoretical questions. For instance, the structure of the second and third peaks constrains the cosmic matter budget*. However, it remains important to improve measurements on larger angular scales as well, both for measuring cosmological parameters and to cross-validate different experiments against potential systematic errors. This is the goal of the present paper.

Since the accuracy of recent measurements leftward of the first acoustic peak is limited by sample-variance rather than instrumental noise, we will use the largest area CMB map publicly available to date with degree scale angular resolution. This map, nicknamed QMASK [9], is shown in Figure 1 and combines the data from the QMAP [10–12] and Saskatoon [13–15] (hereafter SASK sometimes) experiments into a 648 square degree map around the North Celestial Pole. This map has been extensively tested for systematic errors [9], with the conclusion that the QMAP and Saskatoon experiments agree well overall, as well as analyzed for non-Gaussianity [29,30]. However, for the present power spectrum analysis, it is important to perform additional systematic tests to see if there is evidence of scale-dependent problems in any of the maps. In particular, pointing problems, beam uncertainties, sampling and pixelization effects can smear the maps in a way that changes the shape of the power spectrum, suppressing small-scale fluctuations (and under some circumstances boosting the fluctuations as well).

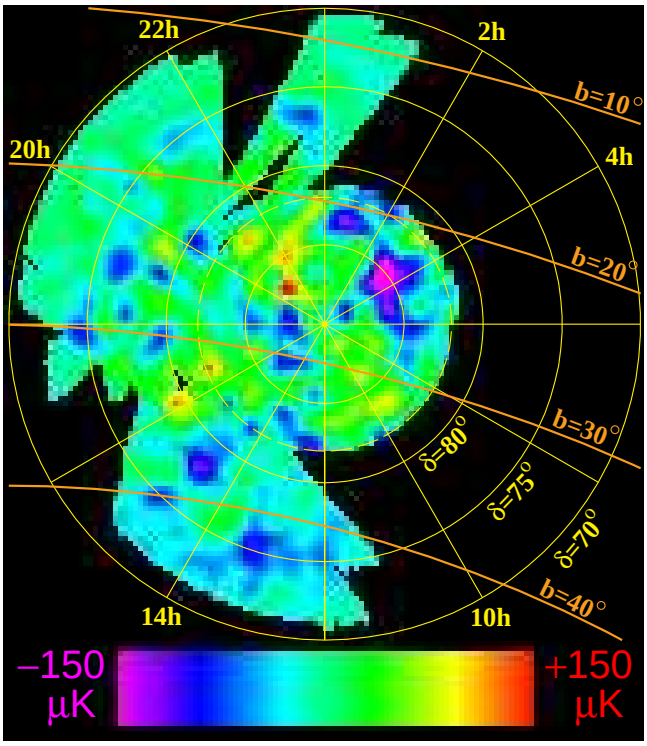

FIG. 1. Wiener-filtered QMASK map combining the QMAP and Saskatoon experiments. The CMB temperature is shown in coordinates where the north celestial pole is at the center of the dashed circle of 16° diameter, with R.A. being zero at the top and increasing clockwise. This map differs from the one published in [9] by the erasing of QMAP information for $\ell \gtrsim 200$ described in the text.

The rest of this paper is organized as follows. In Section II, we present a technique for erasing this type of unreliable information, and apply it to produce a new combined QMASK map where all the statistical weight on small scales comes from Saskatoon. We compute the power spectrum of this combined map in Section III. We discuss systematic errors in section IV, finding good agreement but a hint of suppressed QMAP power for $\ell \gtrsim 200$, and conclude with a rather conservatively cut data set that we believe to be reliable as a starting point for cosmological parameter analysis.

* After this paper was first submitted, accurate new measurements of these higher peaks were reported by the Boomerang [6], DASI [7] and Maxima [8] teams, so we have added comparisons with these results below.

II. COMBINING THE SASK AND QMAP EXPERIMENTS

As will be discussed in more detail in Section IV, pointing problems, beam uncertainties, pixelization and sampling effects can suppress small-scale fluctuations in the CMB power spectrum. The QMAP results may therefore only be valid on large angular scales [10–12]. Both pointing inaccuracies and pixelization effects could have effectively smoothed the QMAP map, suppressing small-scale power. Flight 1 of QMAP [10] was sampled at a relatively low rate, causing the effective beam shapes to be elongated along the scan direction. Since this ellipticity was not modeled in the mapmaking algorithm [12], the resulting smoothing would again be expected to suppress small-scale power. Miller *et al.* [18] present a detailed discussion of these issues, and conclude that the QMAP measurements are likely to be unreliable for $\ell \gtrsim 200$. Although attempts can be made to model and correct for some of these effects, an accurate treatment of the undersampling problem in particular would be way beyond the scope of the present paper, requiring the entire maps to be regenerated from the time-ordered data with an order of magnitude more pixels to be able to resolve the beam ellipticity (the ellipticity is not uniform in direction, since the sky rotated relative to the scan axis during the flights). Such an analysis would hardly be worthwhile anyway, since the strength of QMAP compared to subsequent experiments lies on large scales, not on small scales.

For these reasons, we adopt a more conservative approach, combining the QMAP and Saskatoon maps in such a way that the small-scale QMAP information can be optionally erased as a precaution. By this we do not mean removing the *signal* (smoothing the map), which would just lead to further underestimation of the true power. Rather, we mean removing the *information*, *i.e.*, doing something that causes subsequent analysis steps (like combining with Saskatoon or measuring the power spectrum) to give negligible statistical weight to the small-scale QMAP signal. We achieve this by creating a random map with very large small-scale noise and adding it to the QMAP map, modifying its noise covariance matrix $\mathbf{N}$ accordingly.

In practice, we start by generating a white noise map $\mathbf{x}_{\rm white}$ which has the following properties: it covers the same sky region as QMAP, and each pixel temperature is drawn independently from a Gaussian distribution with zero mean and standard deviation σ, giving it a noise covariance matrix $\mathbf{\Sigma}_{white} = \sigma^2\mathbf{I}$. This makes its angular power spectrum C_ℓ independent of ℓ. We then apply the Laplace operator ∇^2 to the mock map. Since it is pixelized on a square grid, we do this in practice by multiplying by a matrix $\mathbf{L}$ that subtracts each pixel from the average of its four nearest neighbors. The transformed map $\mathbf{x}_{\rm blue} \equiv \mathbf{L}\mathbf{x}_{\rm white}$ thereby obtains a very blue power spectrum $C_\ell \propto \ell^4$, since Laplace transformation corresponds to multiplying by $\ell(\ell+1)$ in the Fourier (multipole) domain. We choose the normalization factor σ such that the blue noise starts dominating the noise and signal of the QMAP map around $\ell \sim 200$. Since the CMB power falls off as $C_\ell \propto \ell^{-2}$, the result is that the added noise is negligible for $\ell < 200$ and dominates completely for $\ell > 300$. Finally, we add this blue noise map to the QMAP map, obtaining

$$\mathbf{x}_{new} = \mathbf{x}_{\rm QMAP} + \mathbf{x}_{\rm blue} = \mathbf{x}_{\rm QMAP} + \mathbf{L}\mathbf{x}_{\rm white}, \quad (1)$$

$$\mathbf{\Sigma}_{new} = \mathbf{\Sigma}_{\rm QMAP} + \mathbf{\Sigma}_{\rm blue} = \mathbf{\Sigma}_{\rm QMAP} + \sigma^2\mathbf{L}\mathbf{L}^{\mathbf{t}}. \quad (2)$$

To quantitatively assess the effect of this procedure, we perform a series of numerical experiments where we rescale the noise level by a factor $p = 0, 1, 3, 5, 7, 1000$. This corresponds to multiplying $\mathbf{x}_{\rm blue}$ by p and multiplying $\mathbf{\Sigma}_{\rm blue}$ by p^2. $p = 0$ means adding no noise, *i.e.*, that $\mathbf{x}_{new}$ retains all QMAP information; $p = \infty$ (or $p = 1000$ in practice) means that $\mathbf{x}_{new}$ contains essentially pure noise. Below we will see that the choice $p = 3$ erases information on small scales $\ell > 200$ very well, while doing little harm on larger scales. After erasing with $p = 3$, we combine the resulting maps with the Saskatoon data as in [9]. The result is shown in Figure 1, and looks almost unchanged (compare Figure 4 in [9]) since Wiener filtering suppresses noisy modes and the smallest scales were noisy to start with.

III. THE ANGULAR POWER SPECTRUM

In this section, we compute the angular power spectrum of the QMASK map produced in the previous section, shown in Figure 1. It contains 6495 pixels and covers a 648 square degree sky region. We calculate the angular power spectrum using the quadratic estimator method of [19,20], implemented as described in [21,22]. This method involves the following steps: (i) S/N compression of data and relevant matrices by omitting Karhunen-Loève (KL) eigenmodes with very low signal-to-noise ratio, (ii) computation of Fisher matrix and raw quadratic estimators, (iii) decorrelation of data points. We compute the power in 20 bands from $\ell = 2$ to 400 of width $\Delta\ell = 20$, which takes about a week on a workstation. We repeated this calculation in its entirity for the following values of the p-parameter: 0 (no information erased), 1, 3, 5, 7 and 1000 (Saskatoon only, QMAP fully erased), as shown in Figure 2.

In the progression of power spectra shown in this figure, the ℓ-values beyond which QMAP is effectively erased is seen to shift to the left as p increases. For $p = 3$, this scale is seen to be of order 200 in the sense that the leftmost points are almost indistinguishable from the $p = 0$ case whereas those with decent signal-to-noise for $\ell \gtrsim 200$ (say points number 10 and 11) are similar to the $p = 1000$ case. Adopting this cutoff scale as our baseline calculation (we further discuss this choice in the next section), we then average these rather noisy

$p = 3$ measurements into six (still uncorrelated) measurements listed in Table 2. The first four probe angular scales where the above-mentioned systematics are likely to be negligible, incorporating the first 9 ℓ-bands (up to $\ell = 180$), and are shown in Figure 3. The horizontal bars show the mean and rms width of the corresponding window functions.

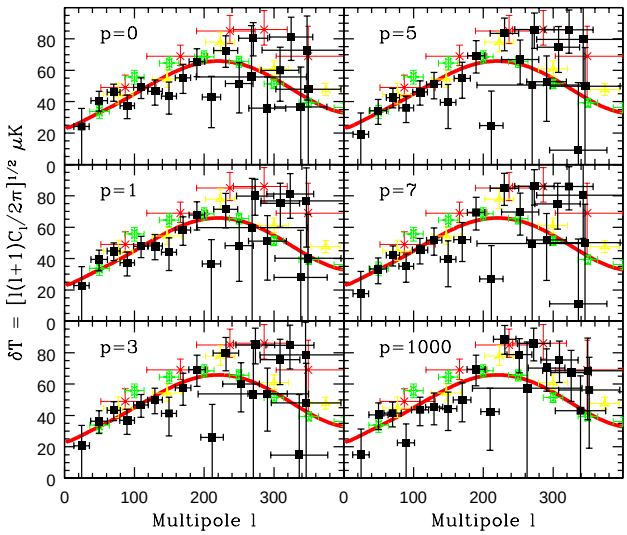

FIG. 2. Angular power spectrum $\delta T \equiv [\ell(\ell+1)C_\ell/2\pi]^{1/2}$ (uncorrelated) in 20 bands of CMB anisotropy from the combined QMASK data in case of $p = 0$(no additional noise at all, just simple combination of SASK and QMAP),1, 3, 5, 7 and 1000 (no QMAP information, only SASK information). For comparison, we also plot the a recent "concordance" model [17] and the power measurements from MAXIMA and BOOMERanG.

$p = 0$		$p = 3$	
ℓ	$\delta T_\ell^2\ [\mu K^2]$	ℓ	$\delta T_\ell^2\ [\mu K^2]$
24 ± 11	641 ± 763	24 ± 11	474 ± 769
49 ± 12	1821 ± 559	49 ± 12	1459 ± 570
70 ± 9	2327 ± 551	70 ± 9	2056 ± 567
90 ± 10	1543 ± 606	90 ± 10	1492 ± 629
110 ± 10	2646 ± 698	109 ± 10	2403 ± 738
130 ± 11	2386 ± 815	130 ± 11	2737 ± 885
150 ± 11	2083 ± 955	150 ± 11	1872 ± 1071
170 ± 11	3358 ± 1108	170 ± 11	3652 ± 1278
190 ± 11	4717 ± 1266	190 ± 11	5265 ± 1487
210 ± 13	2030 ± 1430	211 ± 13	749 ± 1689
231 ± 17	5791 ± 1586	231 ± 17	7007 ± 1861
250 ± 20	2918 ± 1728	253 ± 20	3964 ± 1991
270 ± 21	7116 ± 1865	273 ± 21	7952 ± 2101
291 ± 27	1408 ± 2009	291 ± 27	3207 ± 2211
309 ± 27	3969 ± 2182	309 ± 27	6268 ± 2352
325 ± 31	7263 ± 2421	323 ± 31	7903 ± 2563
339 ± 37	1475 ± 2776	336 ± 37	241.4 ± 2897
349 ± 47	2530 ± 3278	346 ± 47	2540 ± 3378
348 ± 65	5842 ± 3985	345 ± 65	6800 ± 4064
268 ± 79	3430 ± 5187	271 ± 79	3167 ± 5237

Table 1. The power spectra $\delta T \equiv [\ell(\ell+1)C_\ell/2\pi]^{1/2}$ from the QMASK map in two cases:$p = 0$ and $p = 3$. The tabulated error bars are uncorrelated between the twenty measurements, but do not include an overall calibration uncertainty of 10% for δT.

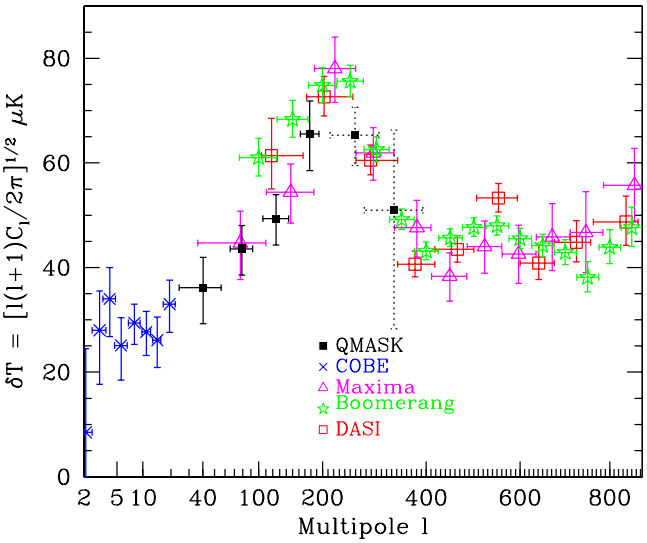

FIG. 3. Uncorrelated measurements of the CMB power spectrum $\delta T \equiv [\ell(\ell+1)C_\ell/2\pi]^{1/2}$ from the combined QMASK data. For comparison, we also plot the measurements from COBE/DMR, MAXIMA, DASI and BOOMERanG. These error bars do not include calibration uncertainties of 10% (QMASK), 10% (BOOMERanG), 4% (DASI) and 4% (MAXIMA). As described in the text, we suggest using only the first four points ($\ell \lesssim 200$), not the two dashed ones, for cosmological model constraints.

ℓ	$\delta T_\ell^2\ [\mu K^2]$
40 ± 16	1308 ± 452
79 ± 13	1899 ± 410
125 ± 19	2436 ± 471
178 ± 15	4295 ± 869
259 ± 46	4265 ± 726
335 ± 58	2596 ± 1795

Table 2. The power spectrum $\delta T \equiv [\ell(\ell+1)C_\ell/2\pi]^{1/2}$ from the QMASK map. The tabulated error bars are uncorrelated between the six measurements, but do not include an overall calibration uncertainty of 10% for δT. We recommend using only the first four for cosmological model constraints.

IV. DISCUSSION

We have measured the CMB power spectrum from the combined QMAP and Saskatoon data sets, obtaining significant detections in the range $\ell \sim 30 - 300$. The key question that we need to address in this section is how reliable these measurements are.

The "usual suspects" as far as systematics and non-CMB contamination are concerned tend to have power spectra that are either redder or bluer than that of the CMB, and therefore naturally split into two categories:

- Problems on *large angular scales* can be caused by contamination from diffuse foregrounds (synchrotron, free-free and spinning dust emission), and systematic errors related to atmospheric contamination, scan-synchronous offsets, atmospheric contamination, *etc.*

- Problems on *small angular scales* can be caused by contamination from point source foregrounds and systematic errors related to pointing problems, beam uncertainties, pixelization and sampling effects.

The foreground contamination [26] has been previously quantified for both Saskatoon [27] and QMAP [28], by cross-correlating the maps in question with a foreground templates tracing synchrotron, dust and free-free emission, point sources, *etc.* The conclusion was that foregrounds contribute at most a few percent to the angular power spectrum reported here, mainly on the largest angular scales. The errors reported on the power spectrum assume that the underlying CMB signal is Gaussian, which is supported by two recent Gaussianity analyses of the QMASK map [29,30].

As opposed to foregrounds, which are true features on the microwave sky, the remaining problems listed above are experiment-specific effects which would be expected to affect QMAP and Saskatoon differently. This provides us with a powerful tool with which to test for their presence, which we will now employ: comparing the QMASK and Saskatoon maps where they overlap.

Previous comparisons between CMB data sets have been done either spatially or in terms of power spectra (discarding phase information). Since two inconsistent maps can have identical power spectra, one should be able to obtain still stronger tests for systematic errors by comparing power *with* phase information. For instance, one could imagine band-pass filtering the two maps to retain only a particular range of multipoles ℓ, and then testing whether these two filtered maps were consistent. We will now describe a simpler way of implementing a test in this spirit.

A. A method for scale-by-scale comparison of two maps

Numerous map comparisons have been performed with the "null-buster" test [16]

$$\nu \equiv \frac{\mathbf{z}^t\mathbf{N}^{-1}\mathbf{S}\mathbf{N}^{-1}\mathbf{z} - \mathrm{tr}\left\{\mathbf{N}^{-1}\mathbf{S}\right\}}{\left[2\,\mathrm{tr}\left\{\mathbf{N}^{-1}\mathbf{S}\mathbf{N}^{-1}\mathbf{S}\right\}\right]^{1/2}}, \tag{3}$$

where ν can be interpreted as the number of "sigmas" at which the difference map $\mathbf{z}$ is inconsistent with pure noise. If the two maps are stored in vectors $\mathbf{x}_1$ and $\mathbf{x}_2$ and have noise covariance matrices $\mathbf{N}_1$ and $\mathbf{N}_2$, then a weighted difference map $\mathbf{z} \equiv \mathbf{x}_1 - \mathbf{r}\mathbf{x}_2$ will have noise covariance $\mathbf{N} \equiv \mathbf{N}_1 + r^2\mathbf{N}_2$. The matrix $\mathbf{S}$ tells the test which modes (linear combinations of the pixels $\mathbf{z}$) to pay most attention to, and can be chosen arbitrarily. The choice $\mathbf{S} = \mathbf{N}$ gives a standard χ^2-test. It can be shown [16] that the null hypothesis that $\mathbf{z}$ is pure noise (that $\langle \mathbf{z}\mathbf{z}^t \rangle = \mathbf{N}$) is ruled out with maximal significance on average if $\mathbf{S}$ is chosen to be the covariance of the expected signal in the map, *i.e.*, $\mathbf{S} = \langle \mathbf{z}\mathbf{z}^t \rangle - \mathbf{N}$. In our case, we choose $\mathbf{S}$ to be the CMB covariance matrix corresponding to a power spectrum

$$\delta T_\ell = \begin{cases} 1\ \mu\mathrm{K} & \text{if } \ell \in [\ell_{min}, \ell_{max}]; \\ 0\ \mu\mathrm{K} & \text{otherwise.} \end{cases}, \tag{4}$$

ensuring that the test only uses information in the multipole interval $[\ell_{min}, \ell_{max}]$. The overall normalization of $\mathbf{S}$ is irrelevant, since it cancels out in equation (3).

B. Results of comparing QMAP and Saskatoon scale-by-scale

We will now use the method described above to compare the QMAP and Saskatoon data scale-by-scale, *i.e.*, in different multipole intervals.

The QMASK map has been shown to be inconsistent with noise at the 62σ level [9]. In the region where the QMAP and Saskatoon maps overlap, they were found to detect signal at 40σ and 21σ, respectively, while the difference map was consistent with pure noise. Which angular scales are contributing most of this information, and how well do the two maps agree scale-by-scale?

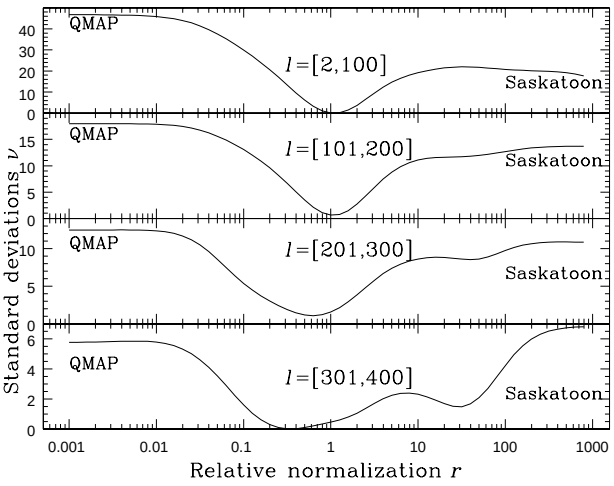

FIG. 4. Comparison of the QMAP and Saskatoon experiments on different angular scales, corresponding to the multipole ranges shown in square brackets. The curves show the number of standard deviations ("sigmas") at which the difference map $\tilde{\mathbf{x}}_{\mathrm{QMAP}} - r\tilde{\mathbf{x}}_{\mathrm{SASK}}$ is inconsistent with mere noise. Note that this is only for the spatial region observed by both experiments.

To answer these questions, Figure 4 shows the result of comparing QMAP with Saskatoon in the four multipole

intervals $[2,100]$, $[101,200]$, $[201,300]$, and $[301,400]$. QMAP is seen to detect signal in the overlap region at 47σ, 18σ, 12σ and 6σ, respectively, whereas the corresponding numbers for Saskatoon are 18σ, 14σ, 11σ and 7σ. In other words, QMAP dominates on large scales, whereas Saskatoon has at least comparable information content on small scales because of superior angular resolution.

Although QMAP and Saskatoon both detect significant CMB signal in all four bands, this signal is seen to be common to both maps since the difference maps $\mathbf{z}$ for $r = 1$ are consistent with noise. Furthermore, there is no evidence of relative calibration errors for the $[2,100]$ or $[101,200]$ bands, since the minima of these two curves are at $r \approx 1$. However, the situation is less clear on smaller scales: the best-fit amplitude of QMAP is only 63% of the amplitude of Saskatoon for $\ell \in [201,300]$, and even lower for $\ell \in [301,400]$. None of these departures of the minimum from $r = 1$ are statistically significant — we cannot determine whether this is a a problem or not simply because the amount of information in the maps drops sharply on small scales where detector noise and beam dilution become important. However, whereas the Saskatoon information was extracted from highly oversampled calculations of the relevant beam patterns on the sky, and should be reliable on small scales, there are a number of reasons why the QMAP data may only be valid on larger ($\ell \lesssim 200$) angular scales [10–12]:

1. The QMAP pointing solution was only accurate to this level [11], and small residual pointing uncertainties could have effectively smoothed the map, suppressing power for $\ell \gtrsim 200$ relative to Saskatoon just as Figure 4 indicates.

2. The QMAP maps were generated by subdividing the sky into square pixels of side $\theta = 0.3125^\circ$, and the effect of this pixelization may well become important on angular scales substantially exceeding $\ell \sim 1/\theta \approx 200$, suppressing power on these scales.

3. Flight 1 of QMAP [10], which dominates the sky coverage in Figure 1 was sampled at a relatively low rate, causing the effective beam shapes to be elongated along the scan direction. Since this ellipticity was not modeled in the mapmaking algorithm [12], the resulting smoothing would again be expected to suppress power on scales $\ell \gtrsim 200$.

Miller *et al.* [18] present a detailed discussion of these issues, and conclude that the QMAP measurements are likely to be unreliable for $\ell \gtrsim 200$. This justifies our $p = 3$ choice in Section 2, effectively discarding this suspect small-scale information from QMAP.

C. Conclusions

We have measured the CMB power spectrum from the combined QMAP and Saskatoon data sets, and performed a number of tests for potential systematic errors. On large angular-scales, $\ell \lesssim 200$, our results appear very solid: foreground contamination has been quantified to contribute no more than a few percent to the power spectrum, and we find beautiful internal consistency between the QMAP and Saskatoon components of our map, both in terms of power amplitude and in terms of spatial phase information. On smaller scales $\ell \gtrsim 200$, there are good *a priori* reasons to discard the QMAP information, and we have therefore done so. Our internal scale-by-scale comparison between QMAP and Saskatoon independently suggests that there may be systematic problems on these scales. Since this unfortunately leaves us with no independent way of validating our Saskatoon results in this small-scale regime, *e.g.*, testing our Saskatoon deconvolution procedure, we strongly recommend the conservative approach of using only the first four band power measurements we have reported in table 2 and Figure 3 — this is also where QMASK is most sensitive relative to other experiments. These four measurements, spanning the range $\ell \sim 30 - 200$, provide among the sharpest and best tested constraints to date on these scales, provide a good starting point for constraining cosmological models.

D. Comparison with other experiments

Figure 2 shows that our results agree well with the "concordance" model of [17]. They are also consistent with BOOMERanG [6], DASI [7] and Maxima [5] once calibration uncertainties are taken into account. The QMAP and Saskatoon calibration uncertainties are $6\% - 10\%$ and 10%, respectively (we have corrected the original δT results [10,14] by a factor 1.05 using the latest Cassiopeia A data [23] as in [24]). Although the uncorrelated components of this may average down somewhat when the two maps are combined, we quote a 10% uncertainty on our result to be conservative. Our results are also consistent with those obtained from QMAP and Saskatoon alone. Our leftmost data point agrees well with the last point measured from COBE/DMR [25] by [19].

The original BOOMERanG98 power spectrum was based on a map area of 436 square degrees [4], so one might expect our error bars on large scales to be a factor $(648/436)^{1/2} \approx 1.2$ smaller. Our actual error bars on δT_ℓ^2 are only about 10% smaller on the best QMASK scales after adjusting for bandwidth differences, which is because of BOOMERanG's lower noise levels (the scan strategy and $1/f$-noise of QMAP introduced a non-negligible amount on noise even on the largest scales). We note that the substantial reduction in error bars relative to the original Saskatoon analysis [14] is due to additional information not only from QMAP, but from Saskatoon as well. This is because our present method extracts all the information present, whereas that employed in [14] was limited to information along radial scans, not using

phase information between scans.

In conclusion, we have measured the CMB power spectrum on angular scales $\ell \sim 30 - 200$ from the QMASK map, placing among sharpest and best tested constraints to date on the shape of the CMB power spectrum as it rises towards the first acoustic peak. Our window functions, the combined map and its noise covariance matrix are available at
www.hep.upenn.edu/ ∼ xuyz/qmask.html.

The authors wish to thank Mark Devlin, Lyman Page and an anonymous referee for useful comments. Support for this work was provided by NSF grant AST00-71213, NASA grants NAG5-9194 and NAG5-11099, the University of Pennsylvania Research Foundation, the Zaccheus Daniel Foundation and the David and Lucile Packard Foundation.

[1] G. F. Smoot *et al.*, ApJ **396**, L1 (1992).
[2] E. Torbet *et al.*, ApJL **521**, L79 (1999).
[3] A. D. Miller *et al.*, ApJL **524**, L1 (1999).
[4] P. de Bernardis *et al.*, Nature **404**, 955 (2000).
[5] S. Hanany *et al.*, ApJL **545**, L5 (2000).
[6] B. C. Netterfield *et al.*, astro-ph/0104460 (2001).
[7] N. W. Halverson, astro-ph/0104489 (2001).
[8] A. Lee T *et al.*, ApJL **561**, L1 (2001).
[9] Y. Xu, M. Tegmark, A. de Oliveira-Costa, M. Devlin, T. Herbig, A. D. Miller, C. B. Netterfield, and L. A. Page, Phys. Rev. D **63**, 103002 (2001).
[10] M. Devlin, A. de Oliveira-Costa, T. Herbig, A. D. Miller, C. B. Netterfield, L. A. Page, and M. Tegmark, ApJL **509**, L77 (1998).
[11] T. Herbig *et al.*, ApJL **509**, L73 (1998).
[12] A. de Oliveira-Costa, M. Devlin, T. Herbig, A. D. Miller, C. B. Netterfield, L. A. Page, and M. Tegmark, ApJL **509**, L77 (1998).
[13] C. B. Netterfield *et al.*, ApJ **445**, L69 (1995).
[14] C. B. Netterfield, M. J. Devlin, N. Jarosik, L. A. Page, and E. J. Wollack; ApJ, **474**, 47 (1997)
[15] M. Tegmark *et al.*, ApJL **474**, L77 (1996a).
[16] M. Tegmark, ApJ **519**, 513 (1999).
[17] M. Tegmark, M. Zaldarriaga, and A. J. S Hamilton, Phys. Rev. D **63**, 043007 (2001).
[18] A. Miller *et al.*, astro-ph/0108030 (2001).
[19] M. Tegmark, Phys. Rev. D **55**, 5895 (1997).
[20] J. R. Bond, A. H. Jaffe, and L. E. Knox, ApJ **533**, 19 (2000).
[21] N. Padmanabhan, M. Tegmark, and A. J. S Hamilton, ApJ **550**, 52P (2001).
[22] M. Tegmark and A. de Oliveira-Costa, Phys. (2001). Rev. D;64;063001
[23] B. Mason *et al.*, Astron. J **118**, 2908 (1999).
[24] E. Gawiser and J. Silk, Phys. Rep. **333**, 245 (2000).
[25] C. L. Bennett *et al.*, ApJ **464**, L1 (1996).
[26] M. Tegmark, D. J. Eisenstein, W. Hu, and A. de Oliveira-Costa, ApJ **530**, 133 (2000).
[27] A. de Oliveira-Costa, A. Kogut, M. J. Devlin, C. B. Netterfield, L. A. Page, E. J. Wollack, ApJ **482**, L17 (1997).
[28] A. de Oliveira-Costa, M. Tegmark, M. J. Devlin, L. M. Haffner Haffner, T. Herbig, A. D. Miller, L. A. Page, R. J. Reynolds, S. L. Tufte, ApJL **542**, L5 (2000).
[29] C. G. Park, C. Park, B. Ratra, and M. Tegmark, ApJ **556**, 582P. (2001).
[30] S. Shandarin, H. Feldman, Xu Y, and Tegmark M, astro-ph/0107136 (2001).